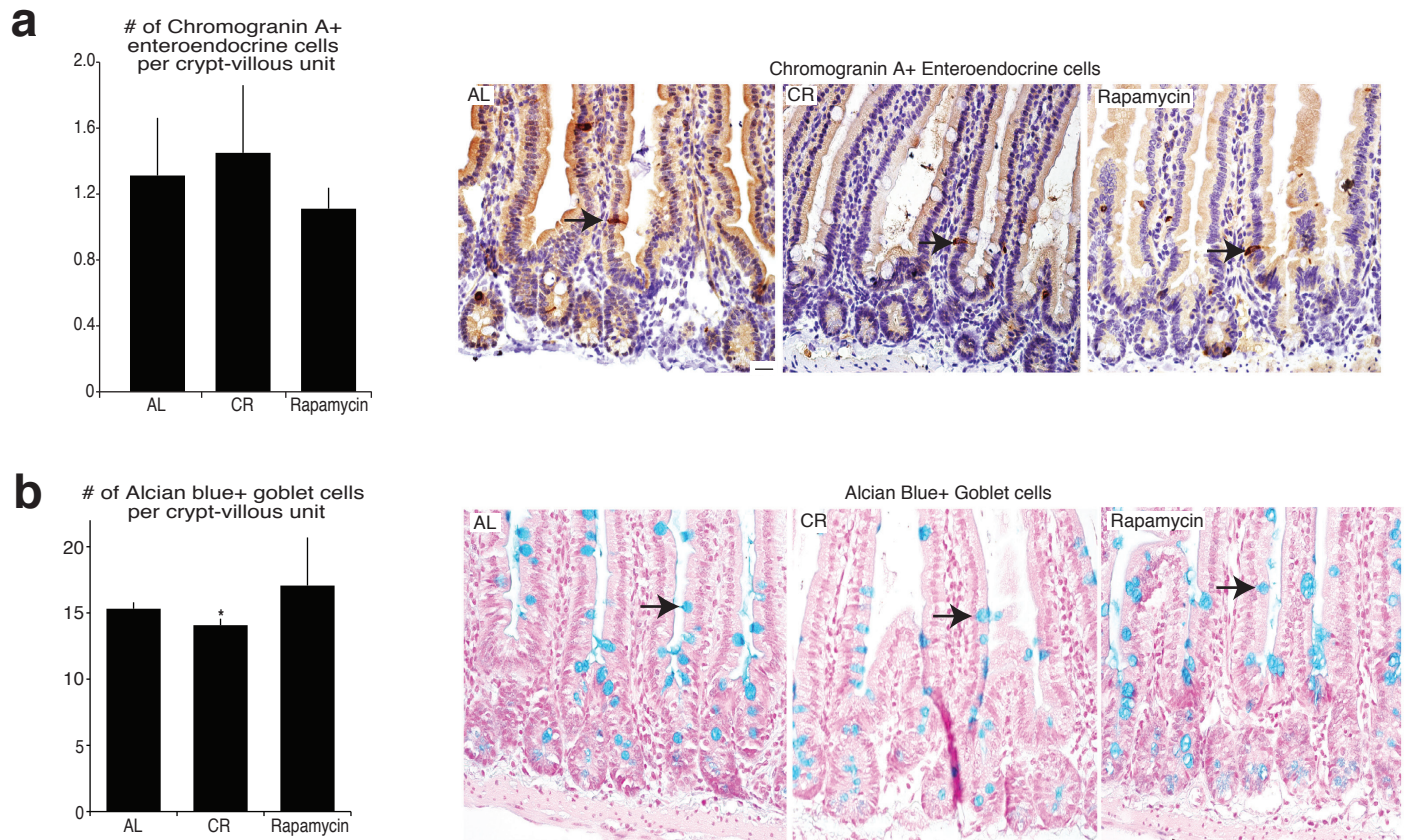


Supplementary Figure 1: Calorie restriction increases the proliferation of ISC but reduces the proliferation and migration of differentiated progenitors into the villi.

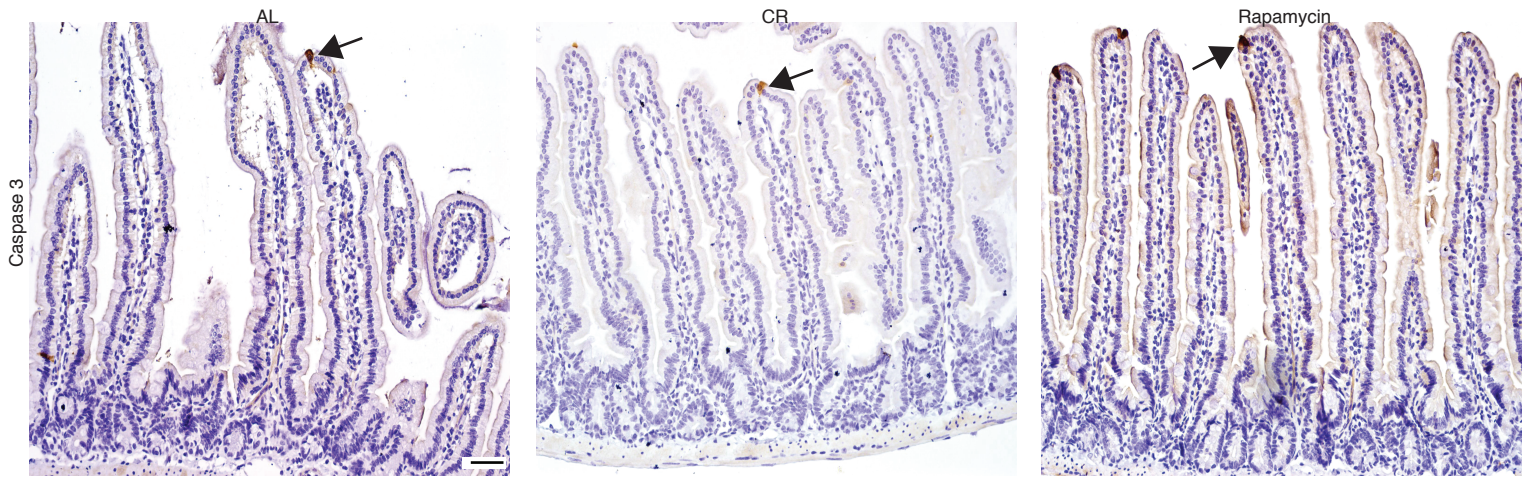
a-f. In comparison to mice on *ad libitum* diet (AL), mice on calorie restriction (CR) lost on average 20% of their mass (a, n=36 and 38), had reduced small intestinal mass (b, n=24 and 29), shorter villi (f, n=6 and 5), and fewer mature villous enterocytes (e, n=3) than AL (n=36). The proximal jejunum was defined as the length between 6 to 9 cm as measured from the pylorus (distal portion of the stomach). CR did not change small intestinal length (c, n=24 and 29) or the density of crypts in the jejunum (d, n=3). **g-h.** CR enhanced the proliferation of Lgr5^{hi} ISCs as assessed 4 hours after a pulse of BrdU assessed in cytopun preparations (h, n=3) and histology (g).

Representative crypts (g) demonstrate increased BrdU positivity in crypt base columnar cells (CBCs, cells adjacent to Paneth cells at the bottom of crypts and designated by arrowheads). **i-k.** Cell migration was determined by administering a single dose of BrdU, which predominantly labels the proliferating transient amplifying cells (TA-cells) that compose most of the crypt, and then mice were sacrificed 24 hours later. 24 hours after a pulse of BrdU (i), CR reduced the migration of labeled BrdU labeled cells into the villi (j, n=3). However, normalized to the total number of villous enterocytes, there is no significant difference in the percentage of BrdU positive cells in CR villi compared to AL controls, indicating that at equilibrium in CR mice TA-cells generate fewer progeny for shorter, less cellular villi (k, n=3). Values are mean, error bars are s.d. * indicates $P < 0.05$ and ** $P < 0.01$, *** $P < 0.001$ scale bar 50 μm



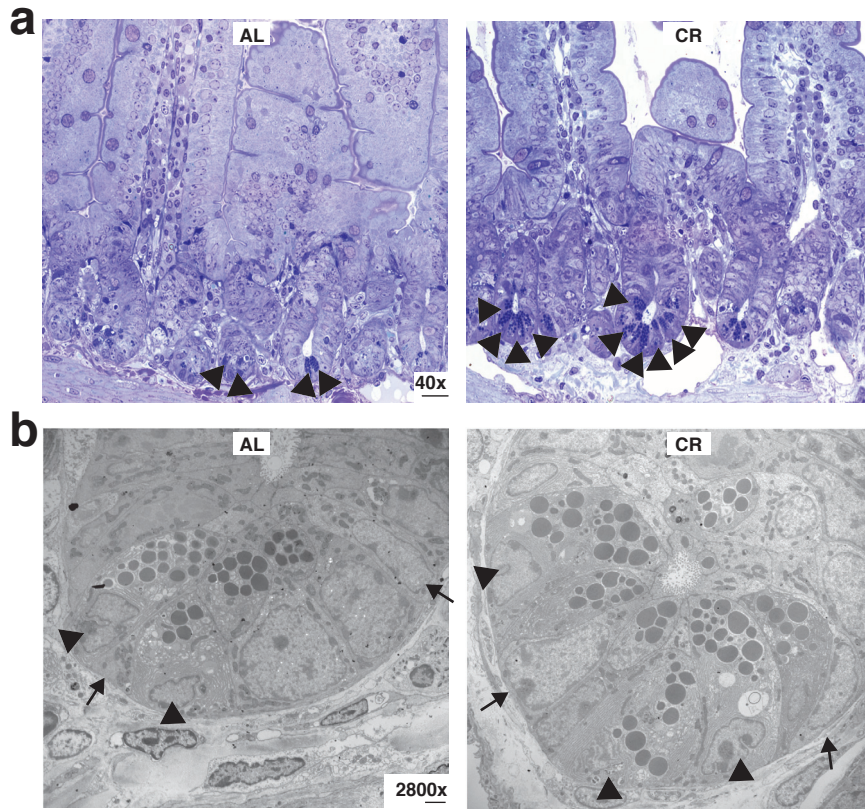
Supplementary Figure 2. Calorie restriction and rapamycin treatment have minimal effects on enteroendocrine and goblet cell differentiation

a. An immunostain for chromogranin A revealed no difference in the numbers of jejunal enteroendocrine cells (arrow) per crypt-villous unit in mice from calorie restriction (CR) (n=5) compared to those in ad libitum (AL) (n=4) fed controls. **b.** An Alcian blue stain showed a mild reduction in mucinous goblet cells (arrow) in CR (n=4) compared to rapamycin treated (n=3) and AL controls (n=4). Values are mean, error bars are s.d. scale bar 20 μ m

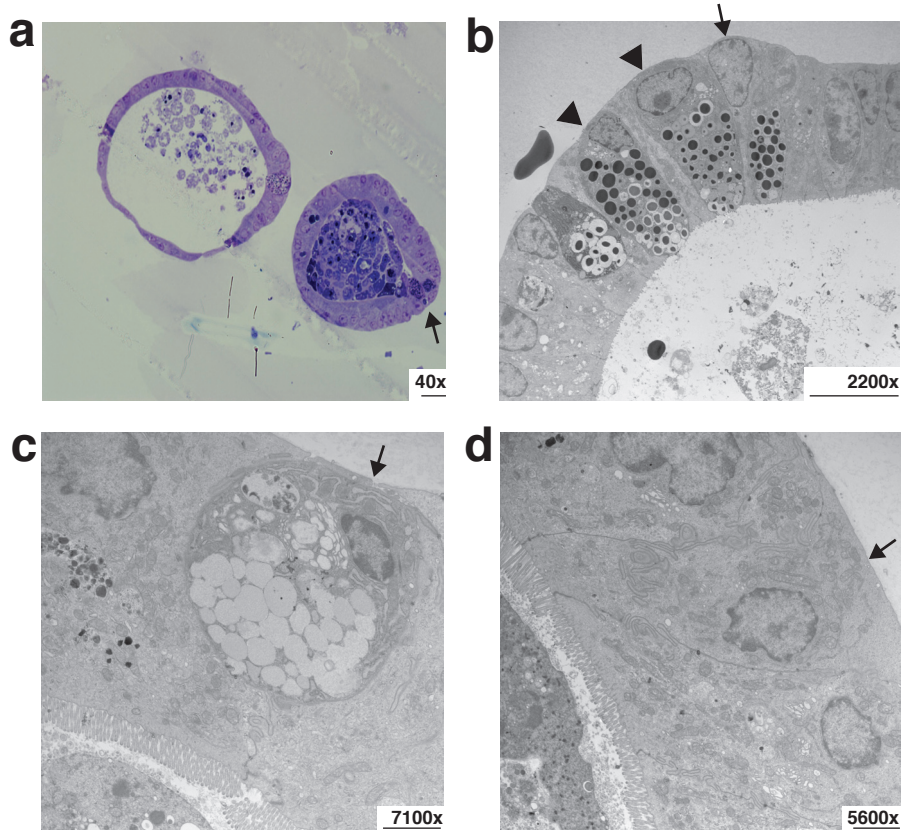


Supplementary Figure 3: Enterocyte apoptosis is not affected by calorie restriction.

Immunostains for cleaved caspase 3 demonstrated no increase by calorie restriction (CR) or rapamycin treatment compared to ad libitum (AL) fed controls. The arrow indicates apoptotic cells at the tips of the villi. (n=3 per group, scale bar 50 μ m)

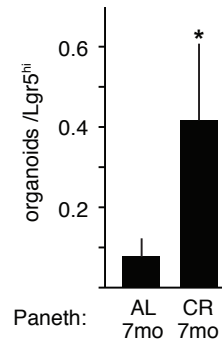


Supplementary Figure 4: Paneth cell ultrastructure is not altered by calorie restriction. **a.** One micron sections of proximal jejunum counterstained with Toluidine Blue revealed increased numbers of Paneth cells (arrowheads) in calorie restriction (CR) compared to ad libitum (AL) fed controls. The proximal jejunum was defined as the length between 6 to 9 cm as measured from the pylorus (distal portion of the stomach). Scale bar 20 μm **b.** Electron microscopy images of representative crypts from AL and CR jejunum demonstrated no differences in the morphologic ultrastructure of crypt base columnar cells (arrow) and Paneth cells (arrowhead). Scale bar 2 μm



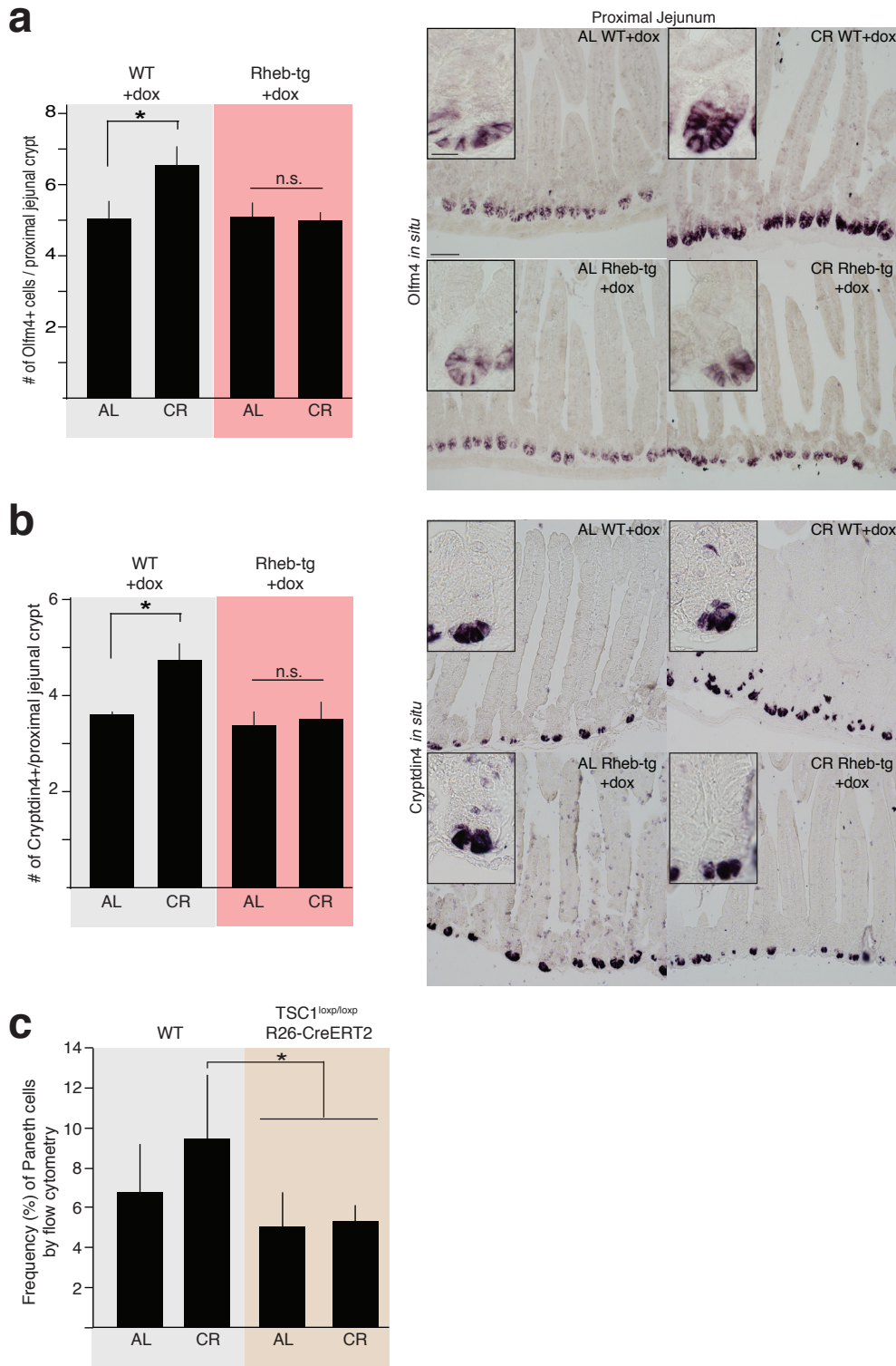
Supplementary Figure 5: Organoid bodies recapitulate normal intestinal morphology and possess all intestinal cell types.

Organoid bodies derived from the coculture of sorted Paneth cells and ISC were harvested after 10 days of incubation. **a.** An H&E-stained section of an organoid body illustrates crypt domains (arrow) and the myriad cell types observed in the small intestine. **b-d.** Electron microscopy images of organoid bodies highlight the various cell types associated with the mammalian small intestine including Paneth cells (b, arrowheads), crypt base columnar cells that are adjacent to the Paneth cells (b, arrow, scale bar 10 μ m), mucinous goblet cells (c, arrow, scale bar 2 μ m), and mature enterocytes with their microvilli (d, arrow, scale bar 2 μ m).



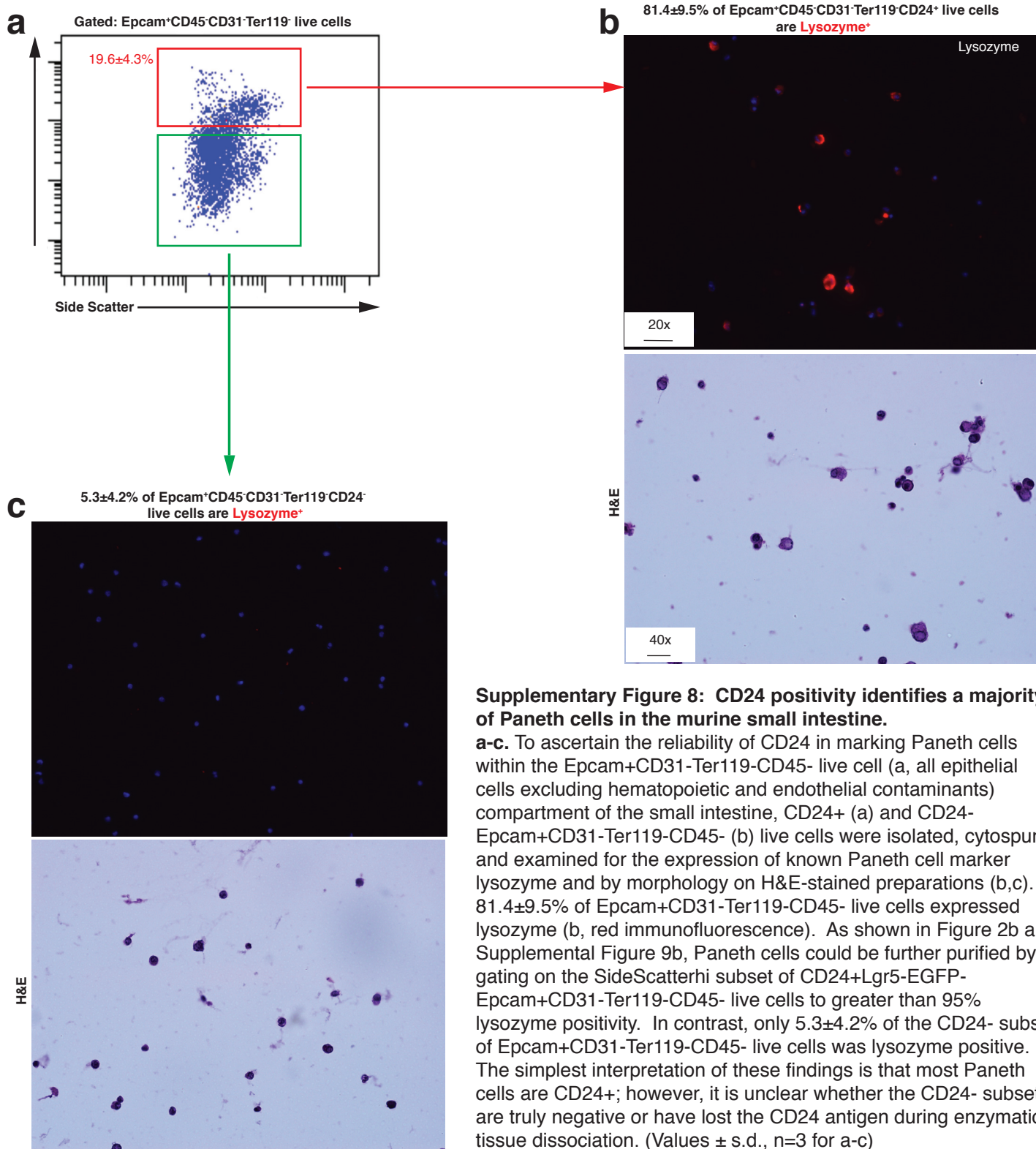
Supplementary Figure 6: Long-term calorie restriction extrinsically augments the capacity of Paneth cells to promote ISC function.

Paneth cells derived from mice on a CR regimen for 7 months extrinsically enhance ISC regeneration in culture. a. Organoid formation per Lgr5^{hi} ISCs (from AL mouse) cocultured with Paneth cells from CR mice was significantly increased compared to Paneth cells from AL mice (n=5).



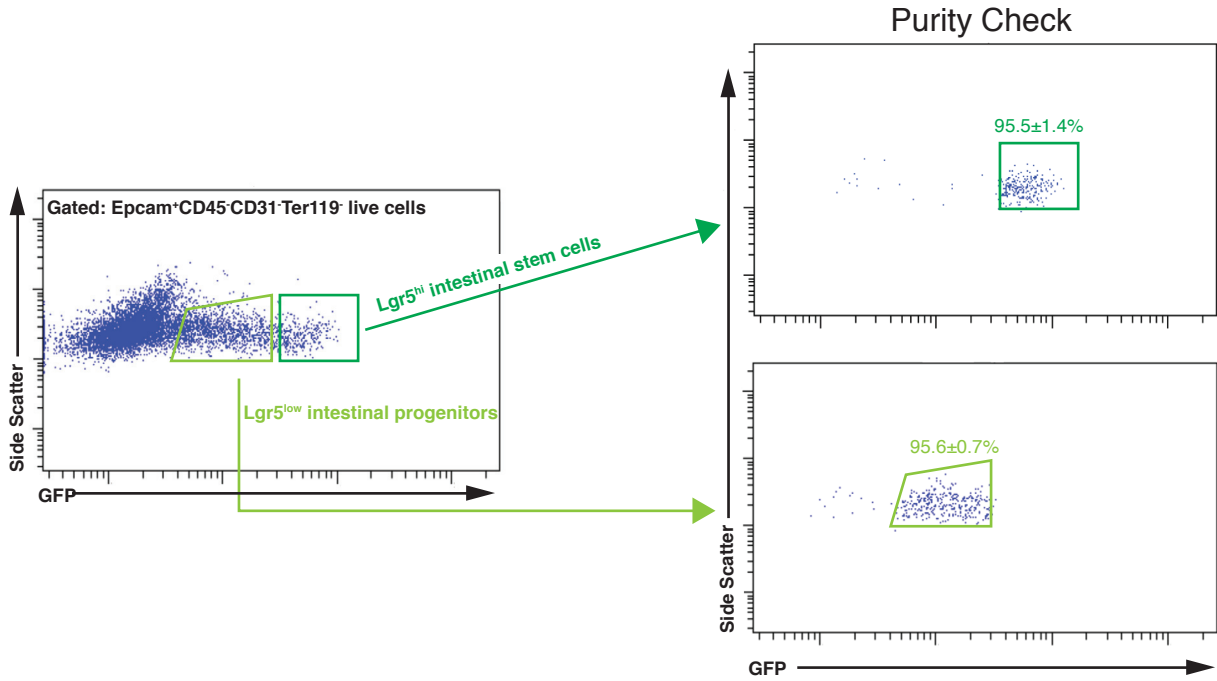
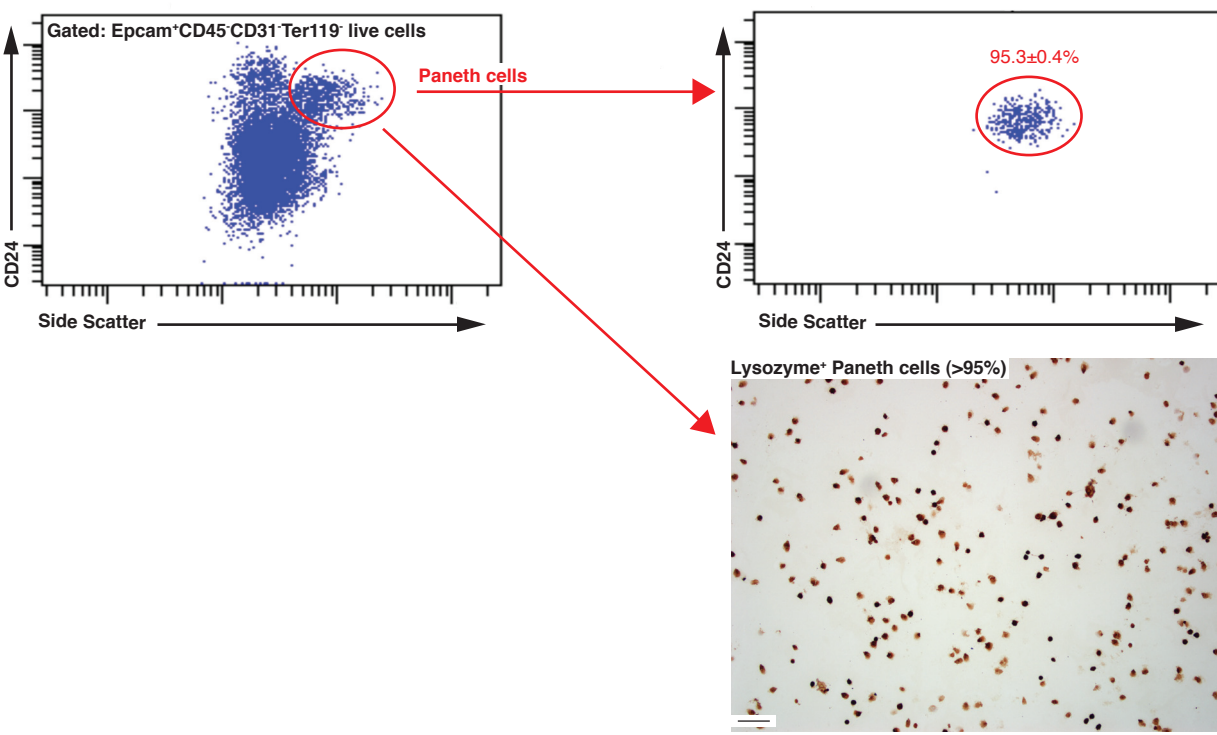
Supplementary Figure 7: Activation of the Rheb2 transgene blunts the increase in intestinal stem cell and Paneth cell frequency that is observed in calorie restriction.

a-b. Calorie restriction (CR) increased the frequency of Olfactomedin-4+ (Olfm4) intestinal stem cells (**a**, ISCs) (n=3) and of Cryptidin4+ Paneth cells (**b**) (n=3 for wt and n=4 for Rheb-tg) by in situ hybridization. This increase in ISCs and Paneth cells was abrogated when the Rheb2 transgene (Rheb-tg) was induced for the duration of CR with doxycycline. Representative images of the proximal jejunum stained for Olfm4 and Cryptidin4 by in situ hybridization. **c.** To independently confirm that persistent mTORC1 activity negated the increase in Paneth cell frequency observed in CR, TSC1—a known negative regulator of mTORC1—was excised using TSC1^{loxp/loxp}; Rosa26(R26)-CreERT2 mice. The excision of TSC1 during CR prevented the increase of Paneth cells (CD24^{hi}SideScatter^{hi}Lgr5-EGFP-Epcam+CD31-Ter119-CD45- live cells) as assessed by flow cytometry. 5 injections of tamoxifen were administered to TSC1^{loxp/loxp}; Rosa26(R26)-CreERT2 mice during the onset of CR and the mice were analyzed 3-4 weeks from the start of CR (n=18 for wt and n=5 for TSC1^{loxp/loxp}). Values are mean, error bars = s.d., * denotes P<0.05, and scale bar 50µm.



Supplementary Figure 8: CD24 positivity identifies a majority of Paneth cells in the murine small intestine.

a-c. To ascertain the reliability of CD24 in marking Paneth cells within the Epcam⁺CD31⁻Ter119⁻CD45⁻ live cell (a, all epithelial cells excluding hematopoietic and endothelial contaminants) compartment of the small intestine, CD24⁺ (a) and CD24⁻Epcam⁺CD31⁻Ter119⁻CD45⁻ (b) live cells were isolated, cytopun, and examined for the expression of known Paneth cell marker lysozyme and by morphology on H&E-stained preparations (b,c). 81.4±9.5% of Epcam⁺CD31⁻Ter119⁻CD45⁻ live cells expressed lysozyme (b, red immunofluorescence). As shown in Figure 2b and Supplemental Figure 9b, Paneth cells could be further purified by gating on the SideScatter^{hi} subset of CD24⁺Lgr5-EGFP-Epcam⁺CD31⁻Ter119⁻CD45⁻ live cells to greater than 95% lysozyme positivity. In contrast, only 5.3±4.2% of the CD24⁻ subset of Epcam⁺CD31⁻Ter119⁻CD45⁻ live cells was lysozyme positive. The simplest interpretation of these findings is that most Paneth cells are CD24⁺; however, it is unclear whether the CD24⁻ subset are truly negative or have lost the CD24 antigen during enzymatic tissue dissociation. (Values ± s.d., n=3 for a-c)

a**b**

Supplementary Figure 9: Intestinal stem cells and Paneth cells can be isolated to near phenotypic purity. a-b. Sorted and analyzed Lgr5-EGFP^{hi} and EGFP^{low}Epcam⁺CD24^{low}-CD31⁺Ter119⁺CD45⁺ live cells were 95.5±1.4% and 95.6±0.7% phenotypically pure, respectively (a, n=3). Similarly, sorted and analyzed CD24^{hi}SideScatter^{hi}Lgr5-EGFP⁺Epcam⁺CD31⁺Ter119⁺CD45⁺ live Paneth cells were 95.3±0.4% phenotypically pure (b, n=3). The SideScatter^{hi} subset of CD24⁺Lgr5-EGFP⁺Epcam⁺CD31⁺Ter119⁺CD45⁺ live cells were greater than 95% Paneth cells based on immunostains for lysozyme, a known Paneth cell marker, in sorted and cytopun preparations. The lysozyme image is a lower magnification of the same side from Figure 2b. Values ± s.d. and scale bar 100µm.